This article was downloaded by: [Renmin University of China]
On: 13 October 2013, At: 10:20
Publisher: Taylor & Francis
Informa Ltd Registered in England and Wales Registered Number: 1072954 Registered office: Mortimer House, 37-41 Mortimer Street, London W1T 3JH, UK

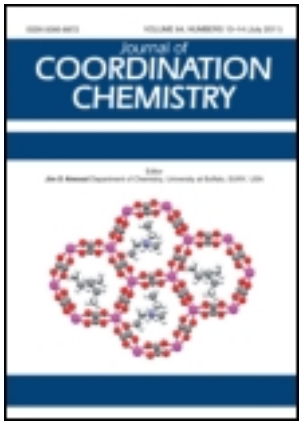

Journal of Coordination Chemistry
Publication details, including instructions for authors and subscription information:
http://www.tandfonline.com/loi/gcoo20

Synthesis, crystal structure, spectroscopy, and nuclease activity of copper(II) complexes containing N,N-bis(2-pyridylmethyl)amine ligand

Jing Qian [a] , Li-Ping Wang [b] , Jin-Lei Tian [c] & Shi-Ping Yan [c]

[a] College of Chemistry, Tianjin Normal University , 300387, Tianjin , P.R. China

[b] Department of Chemistry , Baoding College , 071000, Baoding , P.R. China

[c] Department of Chemistry , Nankai University , 300071, Tianjin , P.R. China

Published online: 25 May 2011.

To cite this article: Jing Qian , Li-Ping Wang , Jin-Lei Tian & Shi-Ping Yan (2011) Synthesis, crystal structure, spectroscopy, and nuclease activity of copper(II) complexes containing N,N-bis(2-pyridylmethyl)amine ligand, Journal of Coordination Chemistry, 64:11, 1991-2001, DOI: 10.1080/00958972.2011.585643

To link to this article: http://dx.doi.org/10.1080/00958972.2011.585643

PLEASE SCROLL DOWN FOR ARTICLE

Taylor & Francis makes every effort to ensure the accuracy of all the information (the "Content") contained in the publications on our platform. However, Taylor & Francis, our agents, and our licensors make no representations or warranties whatsoever as to the accuracy, completeness, or suitability for any purpose of the Content. Any opinions and views expressed in this publication are the opinions and views of the authors, and are not the views of or endorsed by Taylor & Francis. The accuracy of the Content should not be relied upon and should be independently verified with primary sources of information. Taylor and Francis shall not be liable for any losses, actions, claims, proceedings, demands, costs, expenses, damages, and other liabilities whatsoever or howsoever caused arising directly or indirectly in connection with, in relation to or arising out of the use of the Content.

This article may be used for research, teaching, and private study purposes. Any substantial or systematic reproduction, redistribution, reselling, loan, sub-licensing, systematic supply, or distribution in any form to anyone is expressly forbidden. Terms &

Conditions of access and use can be found at http://www.tandfonline.com/page/terms-and-conditions

Downloaded by [Renmin University of China] at 10:20 13 October 2013

Journal of Coordination Chemistry
Vol. 64, No. 11, 10 June 2011, 1991–2001

Taylor & Francis
Taylor & Francis Group

Synthesis, crystal structure, spectroscopy, and nuclease activity of copper(II) complexes containing *N*,*N*-bis(2-pyridylmethyl)amine ligand

JING QIAN*†, LI-PING WANG‡, JIN-LEI TIAN§ and SHI-PING YAN*§

†College of Chemistry, Tianjin Normal University, 300387, Tianjin, P.R. China
‡Department of Chemistry, Baoding College, 071000, Baoding, P.R. China
§Department of Chemistry, Nankai University, 300071, Tianjin, P.R. China

(*Received 6 January 2011; in final form 4 April 2011*)

[Cu(bpea)Cl]ClO_4 (**1**) and a new copper(II) complex [Cu(bpma)(Ph-COO)(H_2O)]ClO_4 (**2**) [bpea = *N*,*N*-bis(2-pyridylmethyl)ethylamine; bpma = *N*,*N*-bis(2-pyridylmethyl)methylamine] have been synthesized. Complex **2** was crystallized in monoclinic space group $P2_1/c$ with unit cell parameters $a = 16.460(6)$ Å, $b = 11.222(4)$ Å, $c = 12.522(5)$ Å, and $\beta = 97.985(6)^\circ$. Interactions of the complexes with calf thymus DNA (CT-DNA) have been investigated by UV absorption, fluorescence, and cyclic voltammetry; thus, modes of CT-DNA binding for the complexes have been proposed. Furthermore, DNA cleavage activities by the complexes were performed in the absence of any external agents. The influence of complex concentration or reaction time on the DNA cleavage was studied.

Keywords: Copper complex; Crystal structure; DNA cleavage; DNA binding

Downloaded by [Renmin University of China] at 10:20 13 October 2013

1. Introduction

The ligands bpa-R, first reported by Romary *et al*. [1], are classical tridentate nitrogen donors in coordination chemistry and have a potential advantage due to the fact that they can bind to the metal both facial and meridional [2] and are more flexible than triazacyclononane (TACN) being strictly facial coordinating [3–5]. Like tris-pyrazolylborates, they can adopt both k2 and k3 coordination modes, but unlike tris-pyrazolylborates they can coordinate in both facial and meridional k3 modes [6]. A large variety of transition metal complexes with bpa-R have been reported [7–17], but studies on copper(II) complexes with bpa-R are relatively limited [18, 19]. Coordination chemistry of copper is a subject of continuing importance, in relation to the structures and reactivity of the active sites in copper metalloproteins [20]. Cu(II), owing to the well-known "plasticity" of the coordination sphere, forms complexes of coordination numbers 4–6, with a variety of irregular geometries [21, 22]. We reported two binuclear copper complexes [23] with bpa-R (bpma, bpea, scheme 1), which display efficient spectroscopic properties. Continuing, we reported a new mononuclear complex with

*Corresponding authors. Email: qianjinger@yahoo.com.cn; yansp@nankai.edu.cn

Journal of Coordination Chemistry
ISSN 0095-8972 print/ISSN 1029-0389 online © 2011 Taylor & Francis
DOI: 10.1080/00958972.2011.585643

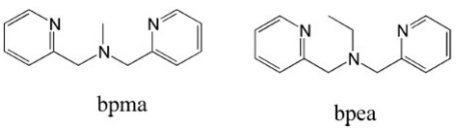

Scheme 1. Structures of ligands.

bpma, [Cu(bpma)(Ph-COO)(H2O)]ClO4 (**2**) and selected a similar reported mononuclear complex for comparison, [Cu(bpea)Cl]ClO4 (**1**) (bpea = N,N-bis(2-pyridylmethyl) ethylamine). DNA cleavage experiments indicate that the complexes cleave DNA efficiently without an external agent.

Downloaded by [Renmin University of China] at 10:20 13 October 2013

2. Experimental

2.1. *Materials and instrumentation*

Caution: Although no problems were encountered in this work, transition-metal perchlorates are potentially explosive and should thus be prepared in small quantities and handled with care.

Unless stated, all reagents used in this research were obtained from commercial sources and used without purification. Solvents used in this research were purified by standard procedures.

Elemental analyses (C, H, and N) were performed on a Model 240 Perkin-Elmer instrument. Infrared (IR) spectra were recorded as KBr pellets from 400 to 4000 cm^{-1} on a Bruker Tensor 27 FTIR spectrophotometer. UV-Vis spectra were measured in CH_3CN solution on a Jasci V-570 UV-Vis spectrophotometer. Electrochemical behaviors of **1** and **2** were investigated by cyclic voltammetry (CV) in CH_3CN containing 0.1 mol L^{-1} $(Bu_4N)PF_6$ as supporting electrolyte. A three-electrode system containing a platinum-wire working electrode, a platinum-plate electrode (counter), and an Ag/AgCl reference electrode was used. Voltammetric recordings were performed under pure nitrogen at room temperature. The concentrations of the complexes were 0.001 mol L^{-1} for each measurement and the voltage scan rate was 50 mV s^{-1}. Electric conductivities were performed on a DDS−11 C conductivity apparatus.

2.2. *Preparation of complexes*

Ligands bpma and bpea were prepared according to literature methods [24, 25].

2.2.1. [Cu(bpea)Cl]ClO_4 (1). To a methanolic solution (10 mL) of bpea (0.5 mmol), an aqueous solution (5 mL) of $CuCl_2 \cdot 6H_2O$ (0.085 g, 0.5 mmol) was added dropwise, and the resulting solution was heated to reflux for 6 h, filtered, and the obtained mixture was added dropwise to a saturated $NaClO_4$ solution, placed in ambient temperature for several days, then stirred for 0.5 h and filtered. Blue block crystals of **1** suitable for X-ray diffraction were obtained by slow evaporation of the filtrate, collected by filtration, washed with diethyl ether, and dried in air. Yield 41% (based on copper salts).

Elemental Anal. Calcd for $C_{14}H_{17}Cl_2CuN_3O_4$ (425.75) (%): C, 39.46; H, 3.99; N, 9.86. Found (%): C, 38.96; H, 3.77; N, 10.21. Complex **1** has been structurally characterized by X-ray crystallography. Selected bond lengths and angles are given in the paper [26].

2.2.2. [Cu(bpma)(Ph-COO)(H_2O)]ClO_4 (2). To an acetonitrile solution (5 mL) of bpma (0.5 mmol), an acetonitrile solution (5 mL) of $Cu(ClO_4)_2 \cdot 6H_2O$ (0.185 g, 0.5 mmol) was added dropwise, the mixture solution was refluxed for 1 h in the presence of air. Then benzyl acid (0.5 mmol)/triethylamine (0.5 mmol) was added and stirred for further 5 h at room temperature and filtered; blue block microcrystals were obtained by quickly evaporating the filtrate overnight and dissolving in H_2O/CH_3OH/DMF (2 : 2 : 1). After 2 weeks, blue block crystals of **2** suitable for X-ray structure analysis were obtained by slow evaporation of the filtrate, collected by filtration, washed with diethyl ether, and dried in air. Yield 49% (based on copper salts). Elemental Anal. Calcd for $C_{20}H_{22}ClCuN_3O_7$ (515.41) (%): C, 46.56; H, 4.27; N, 8.15. Found (%): C, 46.25; H, 4.08; N, 8.39.

2.3. *X-ray structure determination*

The blue prismatic crystal of **2** was mounted on a glass fiber and used for data collection. Crystal data for **2** were collected at 294(2) K using a Bruker Smart 1000 CCD diffractometer. Graphite-monochromated Mo-Kα radiation ($\lambda = 0.71073$ Å) with the ω–2θ scan technique was used. An empirical absorption correction was applied to raw intensities [27]. The structure was solved by direct methods (SHELX-97) and refined with full-matrix least-squares on F^2 using SHELX-97 [28, 29]. Positional and anisotropic atomic displacement parameters were refined for all non-hydrogen atoms. The hydrogens were added theoretically, riding on the concerned atoms and refined with fixed thermal factors. The details of crystallographic data and structure refinement parameters are summarized in table 1.

2.4. *DNA binding experiments*

By the electronic absorption method, the relative bindings of the three complexes to calf thymus DNA (CT-DNA) were studied in 5 mmol L^{-1} Tris-HCl/NaCl buffer at pH = 7.2 (Tris is tris-hydroxy methyl-amino-methane). The solution of CT-DNA gave a ratio of UV absorbance at 260 and 280 nm, A_{260}/A_{280}, of 1.89, indicating that the DNA was sufficiently free of protein [30]. CT-DNA stock solutions of 5 mmol L^{-1} were prepared in Tris-HCl/NaCl buffer, pH = 7.2 (stored at 4°C and used within 4 days after their preparation). The concentration of CT-DNA was determined from its absorption intensity at 260 nm with a molar extinction coefficient of 6600 $(mol\,L^{-1})^{-1}\,cm^{-1}$ [31].

By fluorescence, the relative bindings of the complexes to CT-DNA were studied with an EB-bound CT-DNA solution in 5 mmol L^{-1} Tris-HCl/NaCl buffer (pH 7.2). The excitation wavelength was fixed at 510 nm and the emission range was adjusted before measurements. Fluorescence intensities at 602 nm were measured at different complex concentrations [32].

CV was performed on a BAS Epsilon Electrochemical Workstation with a three-electrode system consisting of a platinum glassy carbon working electrode, a platinum

Downloaded by [Renmin University of China] at 10:20 13 October 2013

Table 1. Crystallographic data and structure refinement parameters for **2**.

Complex empirical formula	$C_{20}H_{22}ClCuN_3O_7$ (**2**)
Formula weight	515.41
Crystal system	Monoclinic
Space group	$P2_1/c$
Unit cell dimensions (Å, °)	
a	16.460(6)
b	11.222(4)
c	12.522(5)
α	90°
β	97.985(6)°
γ	90°
Volume (Å^3), Z	2290.6(15), 4
Calculated density (Mg m^{-3})	1.495
Absorption coefficient (mm^{-1})	1.116
F(000)	1060
θ range for data collection	2.20–25.00
Limiting indices h, k, l	$-19 \le h \le 19$; $-13 \le k \le 13$; $-11 \le l \le 14$
Reflections collected	12,144
Independent reflections	4019 [$R_{int} = 0.1101$]
Data/restraints/parameters	4019/243/289
Goodness-of-fit on F^2	0.997
Final R indices [$I > 2\sigma(I)$]	$R_1 = 0.0890$, $wR_2 = 0.2092$
R indices (all data)	$R_1 = 0.1200$, $wR_2 = 0.2268$
Largest difference peak and hole (e Å^{-3})	0.598/−0.406
CCDC number	760020

wire as the auxiliary electrode, and a saturated calomel electrode (SCE) as the reference electrode. All the electrochemical measurements were carried out in a 10 mL electrolytic cell using 10 mmol L^{-1} Tris-HCl/50 mmol L^{-1} NaCl buffer (pH = 7.2) as the supporting electrolyte. Solutions were deoxygenated by purging with N_2 prior to measurements.

2.5. *DNA cleavage experiments*

The cleavage of supercoiled (SC) pBR322 DNA by the complexes was studied by agarose gel electrophoresis. The reaction was carried out following a literature method [33]. After electrophoresis, bands were visualized by UV light and photographed. The extent of cleavage of the SC DNA was determined by measuring the intensities of the bands using the Gel Documentation System [34]. SC plasmid DNA values were corrected by a factor of 1.22, based on average literature estimate of lowered binding of ethidium [35].

3. Results and discussion

3.1. *Crystal structure*

Complex **2** has been structurally characterized by X-ray crystallography. Selected bond lengths and angles are given in table 2. The crystal structure consists of a mononuclear [Cu(bpma)(PhCOO)(H_2O)] cation and a ClO_4^-, as shown in figure 1. Cu1 is coordinated to a tridentate bpma, a monodentate benzoate, and a water molecule with a square-

Downloaded by [Renmin University of China] at 10:20 13 October 2013

Table 2. Selected bond lengths (Å) and angles (°) for **2**.

Cu(1)–N(1)	1.970(7)	Cu(1)–O(1)	1.936(6)
Cu(1)–N(2)	2.024(8)	Cu(1)–O(3)	2.232(6)
Cu(1)–N(3)	1.969(7)	–	–
O(1)–Cu(1)–N(1)	97.9(3)	N(3)–Cu(1)–N(2)	82.3(3)
O(1)–Cu(1)–N(3)	95.8(3)	O(1)–Cu(1)–O(3)	93.3(3)
N(1)–Cu(1)–N(3)	163.8(3)	N(1)–Cu(1)–O(3)	96.6(3)
O(1)–Cu(1)–N(2)	165.4(3)	N(3)–Cu(1)–O(3)	91.2(3)
N(1)–Cu(1)–N(2)	82.3(3)	N(2)–Cu(1)–O(3)	101.2(3)

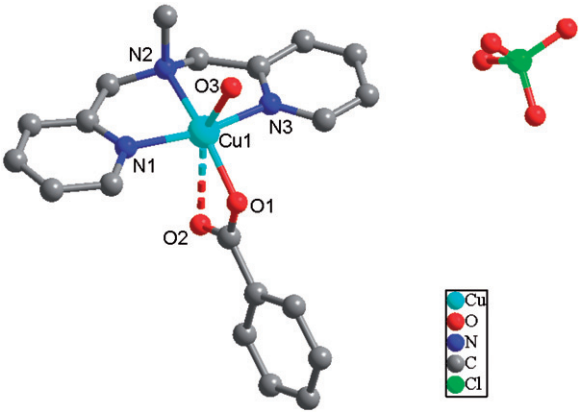

Figure 1. The labeling scheme for $[Cu(bpma)(Ph\text{-}COO)(OH_2)]^-$; hydrogens and ClO_4^- are omitted for clarity.

pyramidal geometry ($\tau = 0.027$) [36, 37] with a $CuN_3O\cdots O$ chromophore (4 + 1). The basal plane is completed by the pyridyl N(1), N(2), and the N(3) of bpa and the O(1) from benzoate. A water molecule occupies the axial position with Cu1–O3 distance of 2.232 Å (longer than Cu1–O1, 1.936 Å). The Cu1 is 0.188 Å out of the square plane formed by N(1), N(2), N(3), and O(1). The Cu–O bond length of 2.084 Å and Cu–N bond average lengths 1.988 Å in the equatorial plane are similar to those found previously [38]. The N1–Cu1–N3 and O1–Cu1–N2 angles are 163.8(3) and 165.4(3)°, respectively. A weak bond exists between O2 and Cu1 with Cu1–O2 distance of 2.614 Å.

3.2. *IR spectrum studies*

The $\nu_{(C-N)}$ of ligand for **2** is a shoulder involving a split sharp peak at 1600 cm^{-1}, while $\nu_{(C-H)}$ is a split sharp peak at 2980 cm^{-1}. Strong absorption, $\nu(ClO_4^-)$, 1094, 1088, and 1031 cm^{-1} are observed, indicating ClO_4^- is uncoordinated. Strong absorptions, ν(benzoate), at 1598, 1557, 1447, and 1394 cm^{-1} are observed. The difference of absorptions exceeds 200 cm^{-1}, indicating benzoate is monodentate to metal ions. This is consistent with structural data of **2**. Additionally, absorptions in the region 620–770 cm^{-1} strongly argue for the presence of pyridyls.

Downloaded by [Renmin University of China] at 10:20 13 October 2013

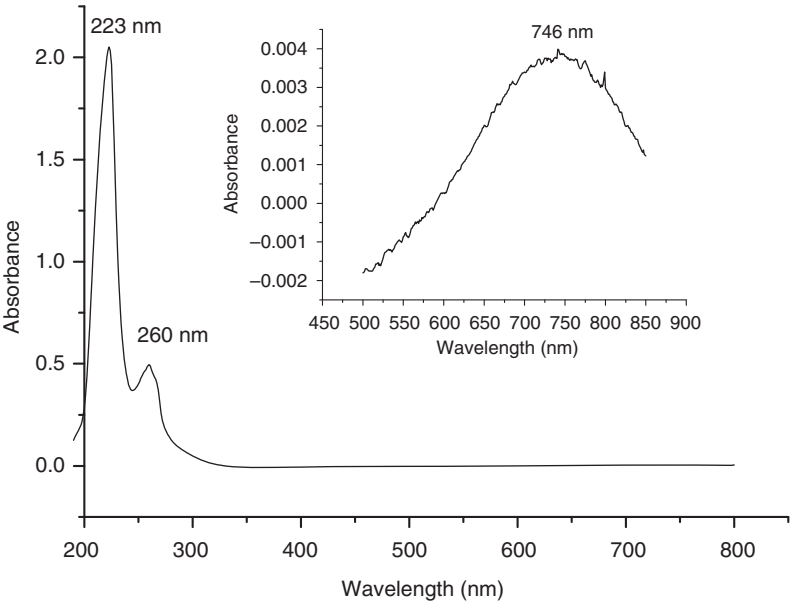

Figure 2. The UV-Vis spectrum of **2** in CH_3CN.

3.3. *Electronic spectrum study*

Electronic absorption spectra in CH_3CN of **2** are shown in figure 2. The very strong absorption in the UV region at 223 nm ($\varepsilon = 2.05 \times 10^4$) can be attributed to π–π^* charge transfer of the ligand. There is also a band at 260 nm ($\varepsilon = 2.17 \times 10^3$). In the visible region the maximum absorption at 746 nm ($\varepsilon = 3.9 \times 10^1$), due to ligand field transition, is consistent with square-pyramidal geometry of Cu(II), typical of d–d transition of Cu(II) in a weak tetragonal ligand field assigned to $d_{x^2-y^2} \rightarrow d_{xy}$, d_{xz}, d_{yz}, d_{z^2} transition. The molar conductivity of **2** in CH_3CN solution is 131 $cm^2\,\Omega^{-1}\,mol^{-1}$. The results are consistent with structural data [39].

3.4. *DNA binding properties*

3.4.1. Spectroscopic titration. DNA binding is the critical step for nuclease activities. Therefore, the binding ability of the complexes to CT-DNA was studied by various techniques. The binding ability of **1** and **2** to CT-DNA was studied by UV spectroscopy by following the intensity changes of the intraligand π–π^* transition band, as shown in figure 3. The absorption at 226 nm for **1** and 223 nm for **2** are attributed to intraligand π–π^* transition; increasing the concentration of CT-DNA, hypochromisms of 27%–38% and red-shifts of 3–20 nm for **1** and **2** were observed. Although this is not definitive proof, hypochromism and red shifts observed for other complexes in the presence of CT-DNA is often a sign of intercalative binding between the aromatic chromophore of the complex and the base pairs of DNA modulate the absorption characteristics of the metal complexes [40]. The values of the intrinsic binding constants (K_b) were determined to be 3.15×10^4 for **1** and 2.84×10^4 for **2** by regression analysis [41].

Downloaded by [Renmin University of China] at 10:20 13 October 2013

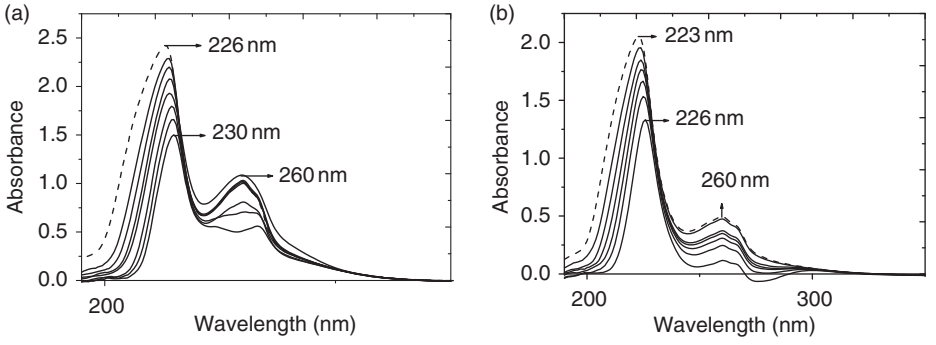

Figure 3. Absorption spectra of **1** (a) (1.20×10^{-4} mol L^{-1}); **2** (b) (3.99×10^{-5} mol L^{-1}) in the absence (dashed line) and presence (solid line) of increasing amounts of CT-DNA (0–4.61×10^{-4} mol L^{-1} of **1** and 0–3.96×10^{-4} mol L^{-1} of **2**) at room temperature in 5 mmol L^{-1} Tris-HCl/NaCl buffer (pH = 7.2). The dashed lines indicate the free complexes.

Downloaded by [Renmin University of China] at 10:20 13 October 2013

The value is ~100 times lower than those reported for classical intercalators (e.g., EB-DNA, $\sim 10^6$ (mol L^{-1})$^{-1}$) [42] and about an order lower than affinities of intercalators containing similar planar ligands [43]. The extent of hypochromism is consistent with the strength of intercalative interaction. The lower K_b observed for the present complexes imply that they do not intercalate very strongly or deeply between the DNA base pairs. So we propose that the lower red shifts observed in the UV spectra are due to the partial/moderate intercalation of pyridyl ligand.

As a means for further clarifying the binding of complexes, fluorescence spectral measurements were carried out. EB does not show any appreciable emission in buffer solution due to fluorescence quenching of the free EB by solvent [44]. EB emits intense fluorescence at 600 nm in the presence of DNA due to its strong intercalation between the adjacent DNA base pairs [45]. It was previously reported that the enhanced fluorescence could be quenched by the addition of another molecule [46]. No luminescence was observed for **1** and **2** at room temperature in aqueous solution or in the presence of CT-DNA, so the binding of the complexes cannot be directly observed in the emission spectra. The relative binding of **1** and **2** to CT-DNA was studied with an EB-bound CT-DNA solution in Tris-HCl buffer (pH 7.2). Fluorescence intensities at 602 nm (526 nm excitation) were measured at different complex concentrations. Figure 4 shows that the fluorescence intensity of EB-bound CT-DNA decreased with the addition of the copper(II) complexes, indicating that the complexes could bind to CT-DNA and replace EB from the EB-bound CT-DNA system. Such a feature is often found in intercalative DNA interactions [47].

3.4.2. Electrochemical study. Figure 5 shows the cyclic voltammograms of **1** and **2** at 50 mV s^{-1}. Both complexes show two couples of waves corresponding to two one-electron redox process of Cu^{II}/Cu^{I} and Cu^{I}/Cu^{0}. The first reduction potentials are observed at $E^1_{pc} = -0.314$ V, $E^1_{pa} = -0.562$ V, and $E^1_{pc} = -0.397$ V, $E^1_{pa} = -0.605$ V for **1** and **2**, respectively; this can be assigned to the redox couple Cu^{II}/Cu^{I}. The second reduction potentials are observed at $E^1_{pc} = -0.497$ V, $E^2_{pa} = -0.891$ V for **1** and $E^2_{pc} = -0.538$ V, $E^2_{pa} = -0.760$ V for **2**; this can be attributed to the redox couple Cu^{I}/Cu^{0}.

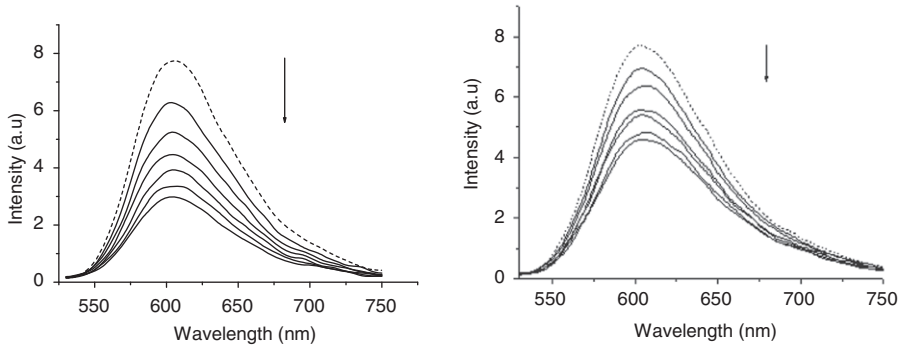

Figure 4. Emission spectra of EB-CT-DNA in the absence (dashed line) and presence (solid lines) of **1** (left), **2** (right) at 293 K.

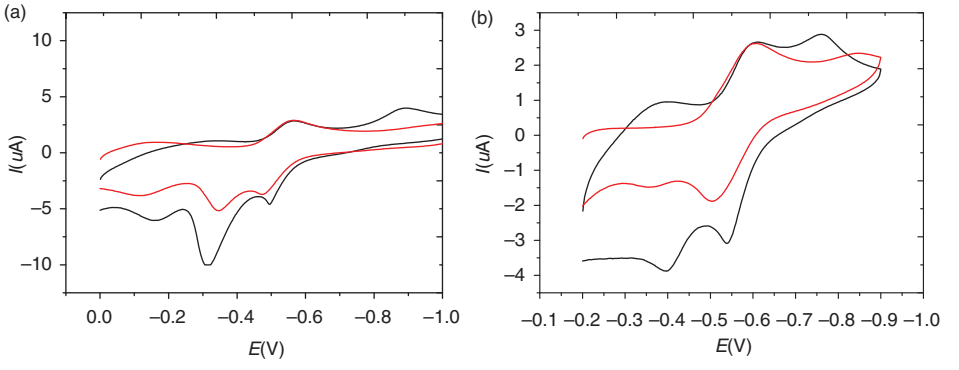

Figure 5. CV of **1** (a) and **2** (b) (0.1 mmol L^{-1} in CH_3CN); scan rate 50 mV s^{-1}; supporting electrolyte $(Bu_4N)PF_6$ (0.1 mol L^{-1}); reference electrode SCE.

The $E_{1/2}$ values are $E^1_{1/2} = -0.438$ V, $E^2_{1/2} = -0.694$ V; $E^1_{1/2} = -0.501$ V, $E^2_{1/2} = -0.649$ V for **1** and **2**, respectively.

In the presence of CT-DNA, the cyclic voltammograms of the two copper(II) complexes exhibited shifts in the cathodic peak potentials followed by a decrease in both peak currents; the $E_{1/2}$ values in the presence of CT-DNA exhibit negative shifts of 15 and 10 mV for **1**, 12 and 17 mV for **2**, indicating interaction between the two copper(II) complexes and CT-DNA. The drop of the voltammetric currents in the presence of CT-DNA can be attributed to diffusion of the metal complex bound to the large, slowly diffusing DNA molecule [48]. The shift in the value of the formal potential ($\Delta E^{0'}$) can be used to estimate the ratio of equilibrium binding constants (K_R/K_O) according to the model of interaction described by Carter and Bard [49]. From this model one can obtain

$$\Delta E^{0'} = E^{0'}_b - E^{0'}_f = 0.059 \log(K_R/K_O),$$

where $E^{0'}_b$ and $E^{0'}_f$ are the formal potentials of the bound and free complex forms, K_R and K_O are the corresponding binding constants for the binding of reduced and oxidized species to CT-DNA, respectively. The $K_{Cu(I)}/K_{Cu(II)}$ values are 1.73 for **1** and

Downloaded by [Renmin University of China] at 10:20 13 October 2013

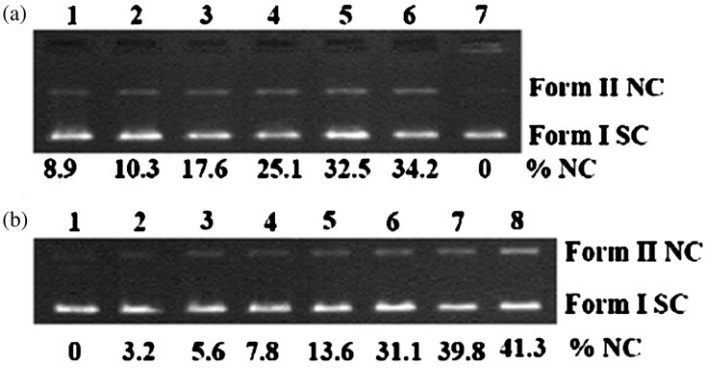

Figure 6. Gel electrophoresis diagrams showing the cleavage of pBR322 DNA (33 μmol L^{-1}) at different complex concentrations in 50 mmol L^{-1} Tris-HCl/NaCl buffer (pH 7.2) and 37°C: (a) Lane 1, DNA control; Lane 2–7: DNA + **1** (0.005; 0.030; 0.072; 0.144; 0.216; 0.252 mmol L^{-1}), respectively; (b) Lane 1, DNA control; Lane 2–8: DNA + **2** (0.003; 0.013; 0.039; 0.078; 0.20; 0.40; 0.50 mmol L^{-1}), respectively.

2.27 for **2**, suggesting stronger binding affinity in the Cu(I) state compared to Cu(II) for both copper(II) complexes.

The values of half-wave potential of the two redox processes and K_{con} measure the relative stability of the Cu^{I} species. The $E_{1/2}$ value cannot be applied to complexes with two copper ions in different coordination environments. However, K_{con} still characterizes the stability of the Cu^{I} species [50]. The values have been determined electrochemically using the equation $\log K_{con} = E_{1/2}/0.0591$ (at 25°C), where $E_{1/2} = E^{1}_{1/2} - E^{2}_{1/2}$. The K_{con} values for the two complexes are calculated to be 2.18×10^{4} and 3.22×10^{2}, respectively, suggesting that the relative stability of the Cu(I) species in **1** is higher than in **2**.

3.5. *DNA cleavage*

The DNA cleavage activity of **1** and **2** has been studied under physiological pH and temperature by gel electrophoresis using SC pBR322 plasmid DNA as the substrate. Figure 6 shows the results obtained at pH 7.2 (Tris-HCl/NaCl) and 37°C for 3 h. In the absence of external agents, the complexes cleave SC DNA (form I) to nicked (form II). The complexes perform DNA cleavage in a concentration-dependent manner. The results indicate that the complexes have potent nuclease activity.

The kinetic parameters underlying the chemistry of the complexes' ability to cleave DNA were determined by following the time dependence of the reaction under pseudo-first-order condition ([complex] = 0.072 mmol L^{-1} of **1** and 0.078 mmol L^{-1} of **2**, and [DNA] = 33 μmol L^{-1} in bp). The loss of SC DNA and increased levels of nicked circular and linear DNA forms were quantified after gel electrophoresis, as described in section 2. The results are shown in figure 7. Complexes **1** and **2** mediate the cleavage of one strand of dsDNA in the initial stage of the reaction. Subsequent nicking was also promoted by the complexes, resulting in the formation of linear DNA.

Downloaded by [Renmin University of China] at 10:20 13 October 2013

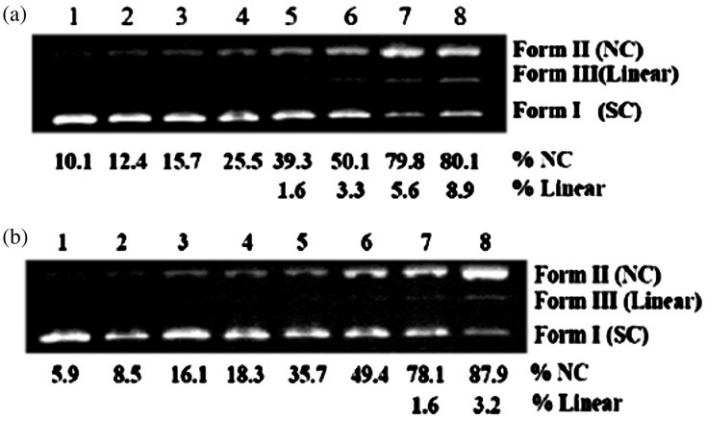

Figure 7. Time-dependence of pBR322 DNA cleavage by 0.072 mmol L^{-1} **1**, 0.078 mmol L^{-1} **2** in Tris-HCl/NaCl buffer (pH = 7.2) at 37°C. (a) Lane 1: DNA control; lane 2–8: DNA + **1** (0.5, 1, 2, 4, 8, 21, 24 h), respectively; (b) Lane 1: DNA control; lane 2–8: DNA + **2** (0.5, 1, 2, 4, 8, 16, 24 h), respectively.

Downloaded by [Renmin University of China] at 10:20 13 October 2013

Acknowledgments

Financial support from the National Natural Science Foundation of China (Grant No. 20771063), the PhD Science Foundation of Tianjin Normal University (Grant No. 52LX28), and Tianjin Educational Committee Foundation (Grant No. 20070606) are gratefully acknowledged.

References

[1] J.K. Romary, J.D. Barger, J.E. Bunds. *Inorg. Chem.*, **7**, 1142 (1968).
[2] S. Pal, M.M. Olmstead, W.H. Armstrong. *Inorg. Chem.*, **33**, 636 (1994).
[3] A.L. Gott, P.C. McGowan, C.N. Temple. *Dalton Trans.*, 1841 (2004).
[4] B. de Bruin, J.A. Brands, J.J.J.M. Donners, M.P.J. Donners, R. de Gelder, J.M.M. Smits, A.W. Gal, A.L. Spek. *Chem.-Eur. J.*, **5**, 2921 (1999).
[5] M.V. Baker, D.H. Brown, B.W. Skelton, A.H. White. *J. Chem. Soc., Dalton Trans.*, 2595 (2002).
[6] S. Thewissen, M.D.M. Reijnders, J.M.M. Smits, B.D. Bruin. *Organometallics*, **24**, 5964 (2005).
[7] J. Mukherjee, V. Balamurugan, R. Gupta, R. Mukherjee. *Dalton Trans.*, 3686 (2003).
[8] A. Hazell, C.J. Mckenzie, L.P. Nielsen. *Polyhedron*, **19**, 1333 (2000).
[9] C. Baffert, I. Romero, J. Pécaut, A. Llobet, A. Deronzier, M.N. Collomb. *Inorg. Chim. Acta*, **357**, 3430 (2004).
[10] M. Ito, Y. Takita, K. Sakai, T. Tubomura. *Chem. Lett.*, 1185 (1998).
[11] S.K. Mandal, W.H. Armstrong. *Inorg. Chim. Acta*, **229**, 261 (1995).
[12] D.R. van Staveren, E. Bothe, T. Weyherműller, N. Metzler-Nolte. *Eur. J. Inorg. Chem.*, 1518 (2002).
[13] M. Rodríguez, I. Romero, A. Llobet, A. Deronzier, M. Biner, T. Parella, H. Stoeckli-Evans. *Inorg. Chem.*, **40**, 4150 (2001).
[14] I. Romero, L. Dubois, M.N. Collomb, A. Deronzier, J.M. Latour, J. Pécaut. *Inorg. Chem.*, **41**, 1795 (2002).
[15] C. Mantel, A.K. Hassan, J. Pécaut, A. Deronzier, M.N. Collomb, C. Duboc-Toia. *J. Am. Chem. Soc.*, **125**, 12337 (2003).
[16] C.E. Dubé, D.W. Wright, S. Pal, P.J. Bonitatebus Jr, W.H. Armstrong. *J. Am. Chem. Soc.*, **120**, 3704 (1998).
[17] S. Thewissen, M.D.M. Reijnders, J.M.M. Smits, B. de Bruin. *Organometallics*, **24**, 5964 (2005).
[18] J. Astner, M. Weitzer, S.P. Foxon, S. Schindler, F.W. Heinemann, J. Mukherjee, R. Gupta, V. Mahadevan, R. Mukherjee. *Inorg. Chim. Acta*, **361**, 279 (2008).

[19] F. Ugozzoli, C. Massera, A.M. Lanfredi, N. Marsich, A. Camus. *Inorg. Chim. Acta*, **340**, 97 (2002).
[20] Y.C. Han, T. Shen, W. Jiang, Q.F. Xia, C.L. Liu. *J. Inorg. Biochem.*, **101**, 214 (2007).
[21] B.J. Hathaway. *Struct. Bond.*, **57**, 55 (1984).
[22] B.J. Hathaway, G. Wilkinson, R.D. Gillard, J.A. McCleverty (Eds). *Comprehensive Coordination Chemistry*, Vol. 5, p. 594, Pergamon Press, Oxford (1987).
[23] J. Qian, J.L. Tian, L. Feng, W. Gu, X.J. Zhao, S.P. Yan. *J. Coord. Chem.*, **62**, 3276 (2009).
[24] S. Pal, M.K. Chan, W.H. Armstrong. *J. Am. Chem. Soc.*, **114**, 6398 (1992).
[25] K.B. Jensen, C.J. Mckenzie, O. Simonsen, H. Toftlund, A. Hazell. *Inorg. Chim. Acta*, **257**, 163 (1997).
[26] O. Yamauchi, T. Yajima, R. Fujii, Y. Shimazaki, M. Yabusaki, M. Takani, M. Tashiro, T. Motoyama, M. Kakuto, Y. Nakabayashi. *J. Inorg. Biochem.*, **102**, 1218 (2008).
[27] G.M. Sheldrick. *SADABS*, *Program for Empirical Absorption Correction of Area Detector Data*, University of Göttingen, Germany (1996).
[28] G.M. Sheldrick. *SHELXS-97*, *Program for the Solution of Crystal Structure*, University of Göttingen, Germany (1997).
[29] G.M. Sheldrick. *SHELXL-97*, *Program for the Refinement of Crystal Structure*, University of Göttingen, Germany (1997).
[30] J. Marmur. *J. Mol. Biol.*, **3**, 208 (1961).
[31] M.E. Reichmann, S.A. Rice, C.A. Thomas, P. Doty. *J. Am. Chem. Soc.*, **76**, 3047 (1954).
[32] B.C. Baguley, M. Le Bret. *Biochemistry*, **23**, 937 (1984); J.R. Lakowiez, G. Weber. *Biochemistry*, **12**, 4161 (1973).
[33] J. Qian, W. Gu, H. Liu, F.X. Gao, L. Feng, S.P. Yan, D.Z. Liao, P. Cheng. *Dalton Trans.*, 1060 (2007).
[34] J. Bermadou, G. Pratviel, F. Bennis, M. Girardet, B. Meunier. *Biochemistry*, **28**, 7268 (1989).
[35] R.P. Hertzberg, P.B. Dervan. *J. Am. Chem. Soc.*, **104**, 313 (1982).
[36] W. Addison, T.N. Rao, J. Reedijk, J. van Rijn, G.C. Verschoor. *J. Chem. Soc., Dalton Trans.*, 1349 (1984).
[37] S.Q. Bai, E.Q. Gao, Z. He, C.J. Fang, C.H. Yan. *New J. Chem.*, **29**, 935 (2005).
[38] H.D. Bian, W. Gu, J.Y. Xu, F. Bian, S.P. Yan, D.Z. Liao, Z.H. Jiang, P. Cheng. *Inorg. Chem.*, **42**, 4265 (2003).
[39] W.J. Geary. *Coord. Chem. Rev.*, **7**, 81 (1971).
[40] E. Yavin Stemp, L. Weiner, I. Sagi, R.A. Yellin, A. Shanzer. *J. Inorg. Biochem.*, **98**, 1750 (2004).
[41] A. Wolfe, G.H. Shimer, T. Meehan. *Biochemistry*, **26**, 6392 (1987).
[42] J.B. Le. Pecq, C. Paoletti. *J. Mol. Biol.*, **27**, 87 (1967).
[43] R.M. Hartshorn, J.K. Barton. *J. Am. Chem. Soc.*, **114**, 5919 (1992).
[44] S. Dhar, M. Nethaji, A.R. Chakravarty. *J. Inorg. Biochem.*, **99**, 805 (2005).
[45] F.J. Meyer-Almes, D. Porschke. *Biochemistry*, **32**, 4246 (1993).
[46] B.C. Baguley, M. Le Bret. *Biochemistry*, **23**, 937 (1984).
[47] C.V. Kumar, J.K. Barton, N.J. Turro. *J. Am. Chem. Soc.*, **107**, 5518 (1985).
[48] X.L. Wang, H. Chao, H. Li, X.L. Hong, L.N. Ji, X.Y. Li. *J. Inorg. Biochem.*, **98**, 423 (2004).
[49] M.T. Carter, A.J. Bard. *J. Am. Chem. Soc.*, **109**, 7528 (1987).
[50] J.P. Lancaster. *The Bioinorganic Chemistry of Nickel*, VCH, New York (1998).

Downloaded by [Renmin University of China] at 10:20 13 October 2013